Morphology of the Eye of the Southern Right Whales (*Eubalaena australis*)

AQ1 **MÓNICA R. BUONO,[1]* MARTA S. FERNÁNDEZ,[2] AND YANINA HERRERA[2]**

[1]Laboratorio de Paleontología, Centro Nacional Patagónico, CONICET, Puerto Madryn, Chubut, Argentina

[2]División Paleontología Vertebrados, Museo de La Plata, CONICET, La Plata, AQ2 Buenos Aires, Argentina

ABSTRACT

Recently, there has been a growing interest in the anatomy and optics of the visual system of cetaceans. However, much of the new information has been focused on odontocetes, and relatively little is known about the visual anatomy of baleen whales. Inthis study, the authors describe the eye anatomy of the southern right whale (*Eubalaena australis*). Eye samples were collected from 26 calves, four adults with known body length, as well as two specimens of unknown body length that had stranded near their nursery ground at Península Valdés, Argentina, over 6 years. The authors provide anatomical descriptions of the eyeball and extraocular structures, as well as quantitative data in the form of eyeball, corneal, scleral, and lens measurements. To explore the sensitivity of the eye to light, the *f*-number was estimated in one specimen. The authors found that the eyes of the calves differed from those of the adults in having less periorbital fat surrounding the eyeball. The authors also observed variations in the abundance of periorbital fat among the adult specimens. The regression analysis revealed a correlation between body length and eyeball size. By contrast, the dimensions of the cornea were only weakly correlated with body length. The estimated *f*-number suggests that the optical sensitivity of the *Eubalaena australis* eye is relatively low. However, caution had to be taken in interpreting *f*-number as a proxy of eye sensitivity because it depends on the lens size, which can be affected by the fixation methods used. Anat Rec, 00:000–000, 2011. ©2011 Wiley Periodicals, Inc.

Key words: *Eubalaena australis*; eye morphology; periorbital fat; optical sensitivity

Abbreviations: CH = dorso-ventral height of the cornea; CW = rostro-caudal width of the cornea; Dpd = diameter of dilated pupil; EH = dorso-ventral height of the eyeball; EL = eyeball length; EW = eyeball; ICA = iridocorneal angle; NMNZ = Museum of New Zealand Te Papa Tongarewa, New Zealand; PND = posterior nodal distance; SMA = standardized major axis.

Grant sponsor: CONICET, Argentina; Grant number: Doctoral research fellowship; Grant sponsor: CONICET, Argentina; Grant number: PIP 0426; Grant sponsor: CONICET, Argentina; Grant number: PIP 2011-2013 to M.T. Dozo; Grant sponsor: Universidad Nacional de La Plata, Programa de Incentivos; Grant number: UNLP N607; Grant sponsor: American Museum of Natural History (Lerner Gray Fund for Marine Research); Grant sponsor: Cetacean Society International (CSI); Grant sponsor: Society for Marine Mammalogy (Grant In Aid of Research); Grant sponsor: FONCyT (Agencia Nacional de Promoción Científica y Tecnológica, Argentina); Grant number: 07/32344.

*Correspondence to: Mónica R. Buono, Laboratorio de Paleontología, Centro Nacional Patagónico, CONICET, Boulevard Brown 2915, Puerto Madryn, 9120, Chubut, Argentina. Fax: +54-2965-451543 E-mail: buono@cenpat.edu.ar

Received 29 June 2011; Accepted 4 October 2011.

DOI 10.1002/ar.21541

Published online 00 Month 2011 in Wiley Online Library (wileyonlinelibrary.com).

J_ID: Z3X Customer A_ID: 11-0178.R1 Cadmus Art: AR21541 Date: 22-November-11 Stage: Page: 2

The morphology of the cetacean eye differs from the typical mammalian eye in several features, such as a thick sclera and cornea, well-developed extraocular muscles and tapetum lucidum, and the flattened anterior segment of the eyeball. These features have been interpreted as adaptations to underwater vision (Wall, 1942; Mass and Supin, 2007). Although several recent publications explore the eye anatomy and functional vision in cetaceans, most of them refer to odontocetes (i.e., Dawson et al., 1972; Herman et al., 1975; Waller, 1982; Dral, 1983; Mass and Supin, 1989; Mass and Supin, 1995; Mass and Supin, 2002; Bjerager et al., 2003; Zhu et al., 2008). Information on mysticete eye morphology and functional vision is comparatively scarce and mainly based on the morphology of adult specimens (Pilleri and Wandeler, 1964; Vasilyevskaya, 1988; Murayama et al., 1992; Mass and Supin, 1997; Zhu et al., 2000; Zhu et al., 2001). In this article, the authors report on the visual morphology of southern right whales (*Eubalaena australis*) of several ontogenetic stages.

The southern right whale is a large baleen whale that inhabits Southern Hemisphere oceans between 20 and 60 degree angle S in latitude and makes annual migrations between higher and lower latitudes (IWC, 2001). In the summer, they move to the feeding grounds in higher latitudes but the location of these areas is uncertain and based mainly on the historic information from whaling records (Townsend, 1935; IWC 2001), strandings, and photo-identified whales on feeding grounds (e.g., Goodall and Galeazzi, 1986; Ohsumi and Kasamatsu, 1986; Best et al., 1993; Best, 1997). Genetic and stable isotope studies have provided insight into their foraging ecology (Best and Schell, 1996; Baker et al., 1999; Rowntree et al., 2008; Valenzuela et al., 2009, 2010). During winter and spring seasons, they return to the nursing grounds where the pregnant females move to nearshore areas to give birth (Payne, 1986; Best, 1990; Patenaude and Baker, 2001).

During the 2003 and 2006 to 2010 seasons, 32 southern right whales stranded on the coasts of Península Valdés (Argentina), permitting us to gather samples from the eyes of calves and adults. Based on these samples recovered by the Stranding Network at Península Valdés, the authors describe their morphology for the first time. As our sample consists of calves and adults, it permits us to explore the morphological differences that can be attributed to the postnatal growth, as well as to compare the morphology of this species with that of the bowhead whale (*Balaena mysticetus*), which has been extensively studied by Zhu et al. (2001).

MATERIALS AND METHODS

Eye samples were collected from 26 calves, four adult right whales and two specimens of unknown body length, which had stranded near the nursery grounds at Península Valdés, Argentina (42-degree angle 30′S, 64-degree angle 10′W), over 6 years (2003; 2006–2010). The eye samples were donated through the Stranding Network at Península Valdés. This is a very large sample, considering the difficulty obtaining right whale specimens, as they are protected endangered species. The eyes were quickly frozen after collecting in a cold room (−20°C) at the Centro Nacional Patagónico, where the eyes were archived in the end of this study. The eyes were studied frozen to avoid the shrinkage of the tissues. Thirty-one specimens were used for anatomical studies, 29 were used for the statistical study, and one was prepared for histological study. Field dissections were conducted only on calves to analyze the extraocular structures *in situ*. Dissections were photographed and observations were recorded as physical notes and drawings. Both eye measurements (taken with a digital caliper Essex ±0.02 mm) and anatomical terminology follow Zhu et al. (2001).

For the histological study, the eye sample 080910-PV-Ea 06 was defrosted and fixed in 8% formalin. This specimen was dissected in cross-section to long axis of body to study the intraocular structures (i.e., cornea, iris, sclera, lens, retina, and choroids). It was then dehydrated in ethanol and embedded in paraffin. Cross-sections of 7 μm were cut on a rotary microtome, mounted onto slides, and stained with hematoxylin, eosin, and Masson's trichrome for routine morphological observation under light microscopy.

To determine the nature of the relationship between the eyeball and corneal sizes and body size (measured as body length), Model II, standardized major axis (SMA) regression analysis were calculated with five different logarithm (base 10) transformed measurements, including: rostro-caudal width of eyeball (EW), eyeball length (axial length, EL), dorso-ventral height of the eyeball (EH), rostro-caudal width of the cornea (CW), and dorso-ventral height of the cornea (CH; Fig. 1). SMA is more F1
appropriate for dealing with allometric approaches (for extensive overviews on the subject, see Warton et al., 2006). Deviations from isometry were assessed by comparing the allometric coefficient with that expected under geometric similarity (Alexander, 1985). Expected coefficients under isometry are equal to 1.0 for variables involved, because they all are linear measurements. Negative allometry refers to the case of a coefficient significantly less than expected by isometry, and positive allometry is when it is significantly higher (Emerson and Bramble, 1993).

To explore the sensitivity of the eye to light, the *f*-number was estimated in a calf (071210-PV-Ea 02). The *f*-number was calculated as the ratio of the focal length of the optical system (=posterior nodal distance, PND; Fig. 1B) to the diameter of the aperture through which light enters (=diameter of dilated pupil, Dpd; Humphries and Ruxton, 2002). As the cetacean eye is emmetropic in water, the PND was measured from the center of the lens to the retina (Mass and Suppin, 2002, 2007). The diameter of the dilated pupil was estimated to be the 90% of the lens diameter (Hughes, 1977). AQ3

RESULTS

Extraocular Structures

In *Eubalaena australis*, like other mysticetes, the eyes are placed laterally in the head behind the angle of the mouth. As in *Balaena mysticetus*, the position of the bulbus oculi (ocular globe or eyeball) is outside of the orbit bone. In two specimens (071210-PV-Ea 02 and 082210-PV-Ea 11), the authors measured the size of the orbit (formed in *E. australis* by the frontal, jugal, lacrimal, maxilla, and squamosal bones) and they compared this with the size of the eyeball. In these specimens, the

ID: selvarajn | Black Lining: [ON] | Time: 14:04 | Path: N:/3b2/AR##/Vol00000/110234/APPFile/JW-AR##110234

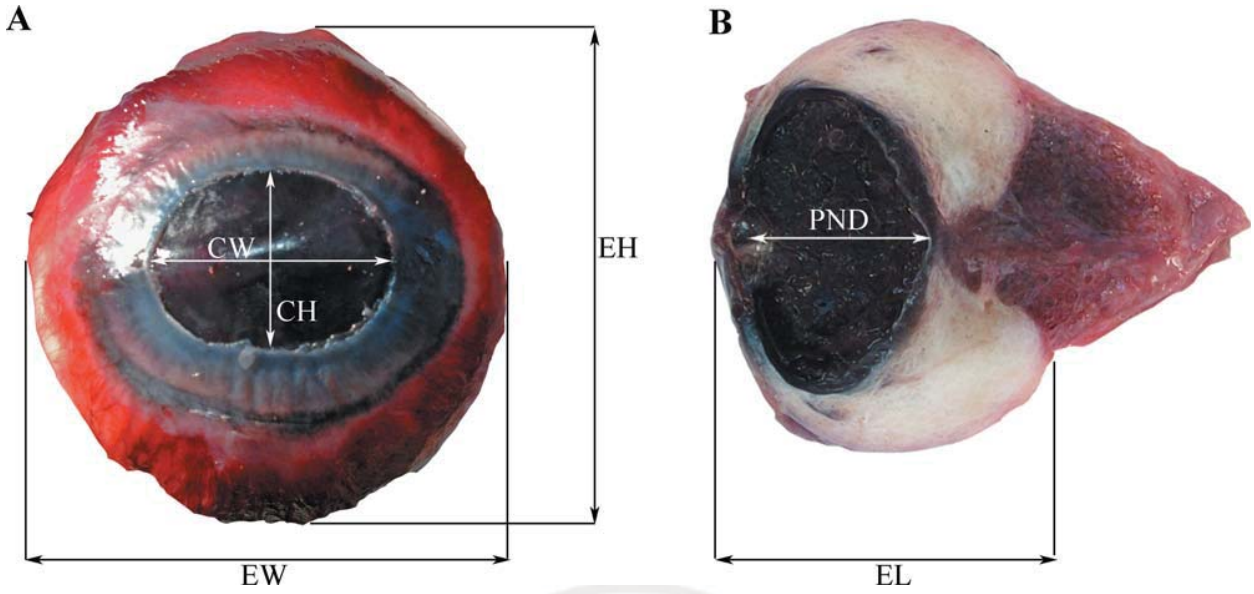

Fig. 1. Anatomical dimensions of *Eubalaena australis* eyeball. **A:** Lateral view of left eyeball; EW, eyeball width in rostro-caudal direction; EH, eyeball height in dorso-ventral direction; CW, corneal width in rostro-caudal direction; CH corneal height in dorso-ventral direction. **B:** Dorso-ventrally transected left eyeball; EL, eyeball length; PND, posterior nodal distance. Without scale.

rostro-caudal width and the dorso-ventral height of the eyeball were 50 and 44% in 071210-PV-Ea 02 and 52 and 67% in 082210-PV-Ea 11, respectively, of the orbit size.

Surrounding the eyeball, the upper and lower eyelids form the margin of the palpebral aperture of the eyeball. The eyelid margins are well defined by two antero-posteriorly oriented furrows. In some specimens, a third and less pronounced furrow are present in the upper eyelid (Fig. 2C). In median section, the skin is thin in the eyelid but thicker in the upper and lower furrows (Fig. 3A). The palpebral aperture, which is the opening of the eyeball, is approximately 1/3 of the palpebral fissure length (Fig. 2A) as has been described for *B. mysticetus* (Zhu et al., 2001). Surrounding the palpebral fissure and located deep in the skin of the eyelids, there are fibers of the orbicularis oculi muscle interspersed in the periorbital fat (Fig. 3B).

Above the eyes, as well as in other regions of the head, the skin of some calves is lighter than in the rest of the head (Fig. 2B). The location of these light gray areas has the same pattern as those of the callosities described in *E. australis* adults (Matthews, 1938; Payne et al., 1983; Reeb et al., 2007) suggesting that skin discoloration precedes the adhesion of amphipod and barnacles colonies.

Zhu et al. (2001, p 732) have described three fatty layers surrounding the eyeball of *B. mysticetus*. The outermost is massive and surrounds the eyeball and orbit, the medium layer is placed between the retractor bulbi muscle and the other extraocular muscles, and the innermost is between the retractor bulbi muscle and the optic nerve sheath. In *E. australis*, there are differences in the development of these fatty layers between calf and adult specimens. In calves, the outermost layer surrounds the orbit giving the shape of a circular structure, which is larger dorsally than ventrally. The thickness of this layer shows variations between the specimens. The structure of this fat is tough and firm, which is related with the abundant amount of collagen fibers and the lack of adipocytes cells that characterize the dermis in *E. australis* (Reeb et al., 2007; Fig. 4A,B). Below this layer, in the hypodermis, fat has a pink coloration by the increase in the vascularization. In some of the calves, there is a thin fatty layer between the retractor bulbi muscle and the bundle that surrounds the optic nerve that corresponds to the inner layer described by Zhu et al. (2001). Anteriorly, it is attached to the sclera in the posterior half of the eyeball and posteriorly to the retractor bulbi muscle. The thickness of this fatty layer is not uniform, showing isolated fat deposits around the retractor bulbi muscle (Fig. 4C,D). It is less tough and firm than the outermost periorbital layer, which could be related to a decrease in the connective tissue and an increase in the adipocyte cells (Reeb et al., 2007). The medium fatty layer has been observed only in three calves (081209-PV-Ea 18, 081709-PV-Ea 19, and 081311-PV-Ea 06; Fig. 4A). The relative thickness of inner and medium layers summed is less than a half of thickness of outermost layer.

By contrast, well-developed medium and inner fatty layers could be identified in only one adult (080310-PV-Ea 05). In this specimen, the innermost fatty layer is thick and well-developed and surrounds the bundle of the optic nerve (Fig. 5). It attaches anteriorly to the sclera. The medium layer was incomplete (due to the extraction of the eye from the orbit) but present and attached anteriorly to the internal side of the palpebral conjunctiva. These two layers have the same soft structure observed in calves. In the other adult specimens

J_ID: Z3X Customer A_ID: 11-0178.R1 Cadmus Art: AR21541 Date: 22-November-11 Stage: Page: 4

Fig. 2. Extraocular structures of the *Eubalaena australis* eye. **A:** Latero-caudal view of left eye of 081411-PV-Ea 07 showing the palpebral aperture and the palpebral fissure (without scale). **B:** Lateral view of the right eye of 082210-PV-Ea 11 showing the light gray areas above the eye, and **C:** the upper and lower eyelids and the three furrows.

(091410-PV-Ea 19; 071910-PV-Ea 01; 102710-PV-Ea33), these layers are very thin and little developed.

Eyeball Anatomy

Eyeball. The shape of the eyeball is not spherical, with the rostro-caudal width and the dorso-ventral height longer than the axial length; as a result the eyeball is flattened latero-medially (Fig. 6D). The mean value of EL:EW and EL:EH is 0.61 in both cases. F6

Conjunctiva. A thin (~0.20 mm in 081709-PV-Ea 09) and delicate bulbar conjunctiva covers the lateral surface of the eyeball and forms a black ring (or gray in some specimens) around the cornea, the pigmented bulbar conjunctiva. Outside of this black ring the bulbar conjunctiva is firmly fixed to the surface of the sclera and is reddish due to high vascularization (Fig. 6C). About ~17 mm (in 081709-PV-Ea 09) from the cornea–sclera junction, the bulbar conjunctiva is thicker and is reflected as palpebral conjunctiva (Fig. 6B). The bulbar conjunctiva consists of stratified epithelium, which toward the lateral surface of the eyeball becomes continuous with the epithelium of the cornea.

Cornea. The cornea is longer rostro-caudally (CW) than dorso-ventrally (CH), with a mean value of CH:CW = 0.71 (Fig. 6C). The corneal outer surface is slightly curved in dorsal view and, as in other cetaceans, is thicker in the periphery than in the center (Table 1). T1 Histologically, the outer epithelium layer was lost prior to fixation but a thin (~15 μm) Bowman layer was identified. The stroma thickness changes from the center (~860 μm) to the periphery (~1,730 μm), containing a large number of collagen fibers, which lie parallel to the corneal surface. A thin endothelial posterior layer composed of flattened cells is present. The Descement's membrane was not identified. Toward the periphery, the cornea joins with the sclera in the limbus.

Sclera. The sclera is the most striking structure of the eye. It surrounds the cornea on the lateral surface of the eyeball and medially to the vitreous chamber and the exit of the optic nerve (Figs. 6D, 7). In transverse F7 section, the sclera is thin toward the corneoscleral junction (6.5 mm in 091410-PV-Ea 19 and 3 mm in 071210-Pv-Ea 02) but thick in medial direction, posteriorly to the vitreous chamber, where it joins with the bundle of the optic nerve (34 mm in 091410-PV-Ea 19 and 24 mm in 071210-Pv-Ea 02) (Fig. 7). The sclera is penetrated by an extensive vascular system that supplies the other structures of the eye (Ninomiya and Yoshida, 2007). In median section through the optic disk, it has numerous vascular vessels, which correspond with the short posterior ciliary arteries. Toward the lateral surface of the eyeball, two long posterior ciliary arteries were identified. In transverse section, one of these vessels is placed in the dorsal margin of the eyeball and the other in the ventral (Fig. 7). Histologically, the sclera is composed of an innermost dense connective tissue layer with a large amount of collagen fibers embedded within the substantia propria. These fibers are tightly packed and arranged in different directions to each other, which gives strength and shape to the eyeball (Fig. 8A). The F8 thickness of this layer increases in the medial direction.

COLOR

ID: selvarajn | Black Lining: [ON] | Time: 14:04 | Path: N:/3b2/AR##/Vol00000/110234/APPFile/JW-AR##110234

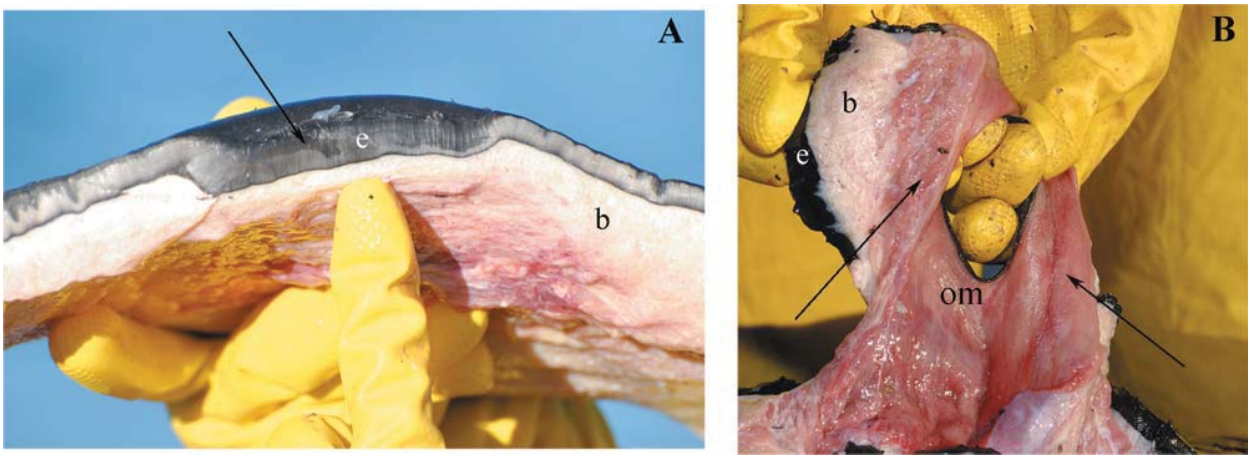

Fig. 3. **A:** Longitudinal section through the upper furrow showing the thickening (arrow) of the skin. **B:** Median view of the eyelids with the fibers of the orbicularis oculi muscle surrounding the palpebral fissure (arrows). Epidermis (e); blubber; (b) orbicularis oculi muscle (om). Specimen number 081010-PV-Ea 09.

The outermost layer, the lamina episcleralis, consisted of loose connective tissue with more abundant blood vessels. Large amounts of pigmented cells were identified in the sclerocorneal stroma of the limbus. In the iridocorneal angle (ICA), the sclerocorneal stroma presents a meshwork of trabeculae and the spaces of Fontana covered by a thin endothelium layer (Fig. 8B). This system of trabeculae and spaces is responsible for draining aqueous humor toward the ICA.

Iris and ciliary body. The iris is a thin, elastic, and black membrane that is placed between the anterior chamber and the lens. The central aperture forms the pupil, which is almost spherical. Histologically, the iris is formed by the outer limiting layer, stroma, sphincter papillae muscle, dilator papillae muscle, and the inner iris epithelium (Fig. 8C). The outer limiting layer extends from the pupil margin to the periphery of the iris. It consists almost entirely of melanocytes, which increase in number toward the pupil margin. The thick stroma underlies this layer, with a large amount of blood vessels and melanocytes interspersed in the loose connective tissue. The iris stroma is supplied by ramifications of the major arterial circle and iridic arteries (Ninomiya and Yoshida, 2007). The inner iris epithelium is placed toward the vitreous chamber and is formed mainly by melanocytes. A well-developed dilator papillae muscle is placed between the stroma and the inner iris epithelium. This thick layer (80 μm) extends from the pupil margin to approximately 1/3 of the iris length. The sphincter papillae muscle could not be identified. Toward the periphery, the iris is continuous with the ciliary body. This is a triangular structure histologically defined by an inner ciliary epithelium and an outer stroma. The ciliary epithelium is composed of a thin inner layer (∼15 μm) of nonpigmented cell, and a thick outer layer (∼30 μm) with abundant melanocytes. The thick stroma consists of connective tissue with a large amount of blood vessels, which corresponds with ramifications of the radial iridic artery and collecting venules (Ninomiya and Yoshida, 2007). Toward the vitreous chamber, there are numerous folds composed of the ciliary epithelium and the stroma, which correspond with the ciliary processes (Fig. 8B). The ciliary muscles could not be identified.

Lens. The lens is almost spherical and is suspended between the iris and vitreous chamber by the zonular fibers (Fig. 7). The capsule and the epithelium in the anterior region of the lens were lost prior to the fixation. Only the epithelium in the equator region of the lens, composed of cuboids cells, was identified. The nucleus lens consists of latero-medially oriented elongate and parallel fiber cells.

Vitrous chamber. The vitrous chamber is larger dorso-ventrally than latero-medially giving the characteristic cetacean eyecup shape close to a hemisphere (Mass and Supin, 2007). The vitrous chamber is filled by the viscous vitreous body (Fig. 7).

Retina and choroid. The characteristic seven layers of the retina were identified. The retinal thickness is ∼230 μm. The choroid is extensively vascularized layer, and it lies behind the retinal epithelium. The stroma is composed of abundant blood vessels, associated with the inner surface of the choroid, which corresponds to the ramification of the choroidal arteries and veins (Ninomiya and Yoshida, 2007). Melanocytes are scattered within the connective tissue of the choroid stroma. The tapetum lucidum is well-developed and has a gray–blue coloration.

Optic nerve. The optic nerve exits the eyecup in the optic disk. At this point, it is enveloped by the sclera and, to a lesser degree, by the ophthalmic rete. The diameter of the optic nerve at the exit of the eyecup is 5.90 mm in 091410-Pv-Ea19 and 3.1 mm in 082110-Pv-Ea 10. In the medial direction, the ophthalmic rete is more developed, forming a cone shaped-structure that surrounds the optic nerve (Fig. 7). The ophthalmic rete forms a network of arterial and venous vessels which

J_ID: Z3X Customer A_ID: 11-0178.R1 Cadmus Art: AR21541 Date: 22-November-11 Stage: Page: 6

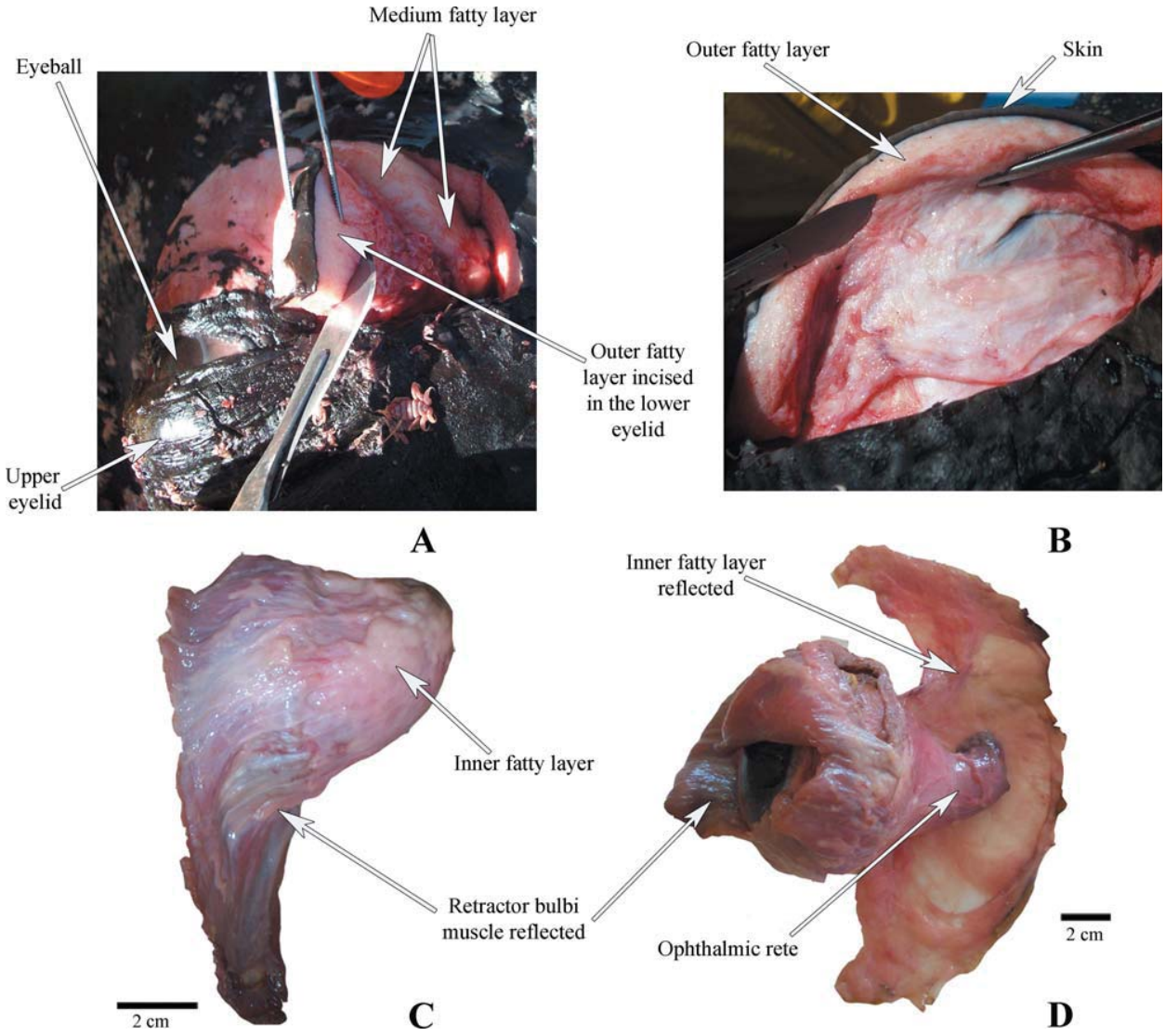

Fig. 4. **A:** Dissection of the right eye region of the calf 081311-PV-Ea 06 viewed from the dorso-caudal aspect of the head. The outer fatty layer of the lower eyelid is incised to expose the deeper medium fatty layer. **B:** Dorsal aspect of the orbital region in the same specimen with the outer fatty layer of the upper eyelid incised and reflected. **C:** Caudal view of the eyeball of 081709-PV-Ea 19 with the retractor bulbi muscle reflected showing the poorly developed inner fatty layer. **D:** Latero-caudal view of the eyeball of 081709-PV-Ea with the inner fatty layer reflected. Note the difference in the structure between the outermost fatty layer more tight and firm than the innermost fatty layer.

COLOR

present with different calibers and are dispersed in abundant connective tissue (Fig. 8D). Only in 080310PV-Ea 05 was a well-developed fat deposit identified interspersed in this region (Fig. 5). The ophthalmic rete is less developed toward the optic foramen. At this point, the optic nerve is enveloped only by a fibrous sheath.

Relative Size of the Eye and its Components

F9 Data for 29 specimens are given in Table 1. Figure 9 shows as logarithmic plots, how the length, width, and height of the eyeball and corneal width correlate with body length. Of the three linear measurements of the eyeball, treated as logarithms, the body length correlates best with the eyeball height and width ($r = 0.92$) and least with the axial length ($r = 0.79$). On one hand, the corneal width and body length have a weaker relationship with $r = 0.49$. On the other hand, the relationship between body size and corneal height is not significant (Table 2). The regressions of eye length, width, and height on body length reveal a negatively allometric relationship between eye size and body size (Table 2). T2

Lens Size and *f*-Number

Lenses sampled, excepting for one specimen, showed aberrations (i.e., shrinkage, deformation, and decomposition) due to having been frozen. However, in one calf

ID: selvarajn | Black Lining: [ON] | Time: 14:04 | Path: N:/3b2/AR##/Vol00000/110234/APPFile/JW-AR##110234

J_ID: Z3X Customer A_ID: 11-0178.R1 Cadmus Art: AR21541 Date: 22-November-11 Stage: Page: 7

dissected (071210-Pv-Ea 02), the lens was in good condition and some optical parameters were estimates. The rostro-caudal width and the dorso-ventral height of the lens are 10 and 11 mm, respectively. The focal length (PND) is 18 mm resulting in an *f*-number of 2 and 1.81 depending upon lens diameter used.

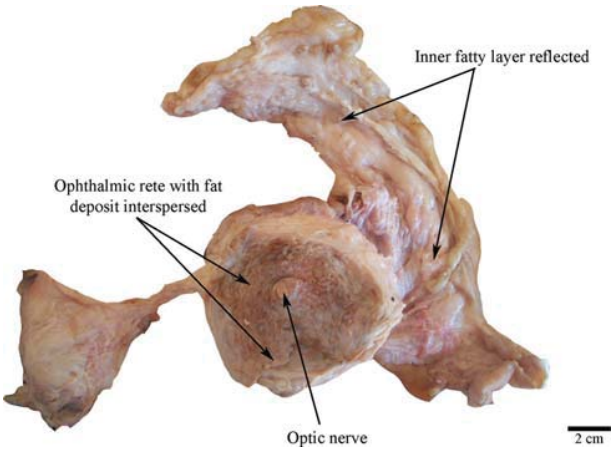

COLOR

Fig. 5. Medial view of the left eyeball of the adult 080310-PV-Ea 05 showing the well-developed inner fatty layer and the fat deposit interspersed in the ophthalmic rete.

DISCUSSION

The southern right whale eye resembles morphologically and histologically that of other mysticetes, particularly that of bowhead whales. The thick sclera, absence of ciliary muscles, highly developed vascular rete, and well-developed choroid and tapetum lucidum, are typical features of the cetacean eye (Mass and Supin, 2007). The functional implication of a thickened sclera, also found in sharks, marine turtles and other marine mammals, still remains unclear. Some authors proposed that it helps to avoid deformations of the eyeball produced by the high pressure during diving or during the retraction into the orbit (Dawson, 1980; Kastelein et al., 1990; Zhu et al., 2001; Bjerager et al., 2003). Another explanation for thickened sclera is the need for a nonspherical globe to maintain peripheral rigidity and prevent deformation of the cornea at differential pressures. This hypothesis, based on the analysis of the ocular morphology of the diving Leatherback sea turtle

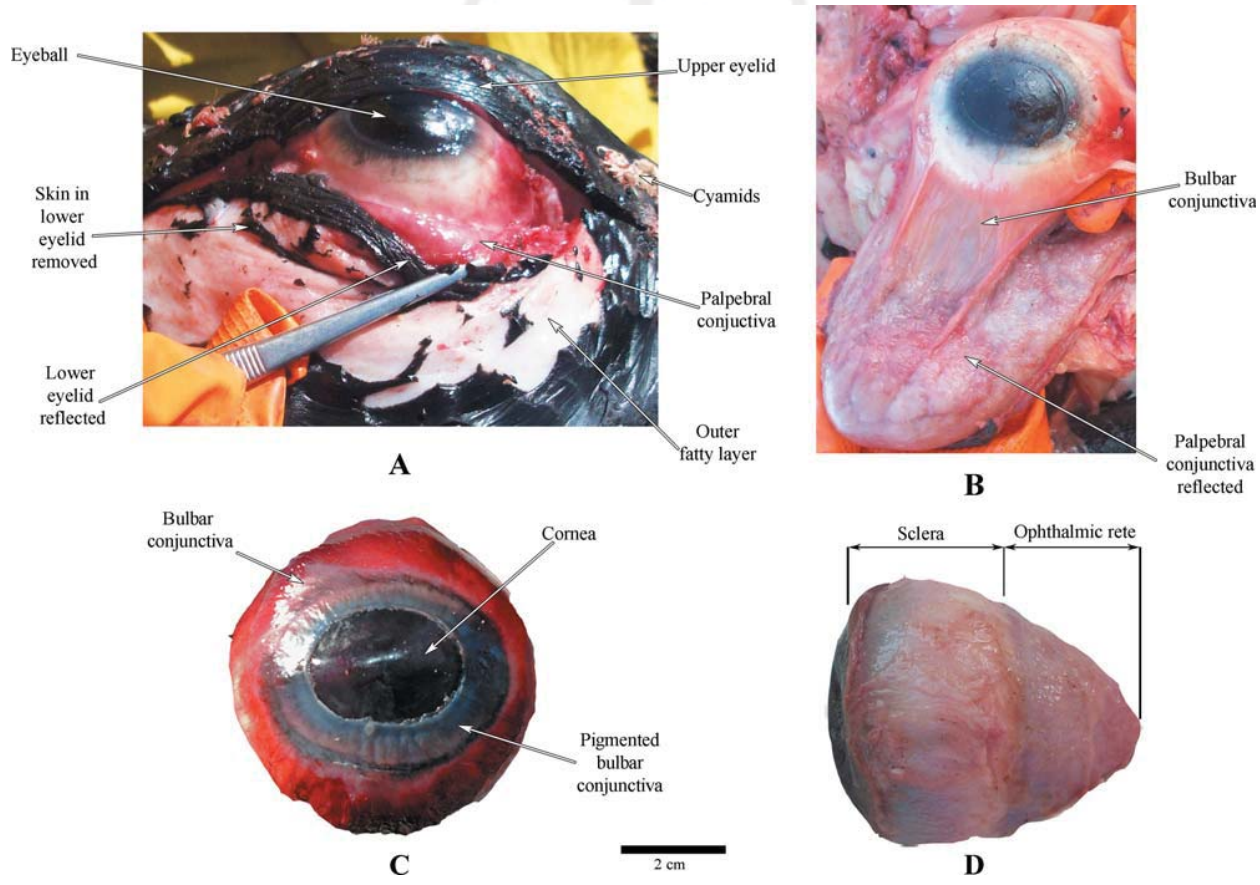

COLOR

Fig. 6. **A:** Ventral view of the dissected right eye of the calf 081311-PV-Ea 06 showing the palpebral conjunctiva attached to the internal side of the lower eyelid, and **B:** the bulbar conjunctiva attached to the sclera. **C:** Lateral view of left eyeball of the calf 082711-PV-Ea 15 illustrating the cornea and the bulbar conjunctiva pigmentation. **D:** Caudal view of left eyeball of calf 082210-PV-Ea 11 showing sclera and ophthalmic rete. (A) and (B) without scale.

AQ4

ID: selvarajn | Black Lining: [ON] | Time: 14:05 | Path: N:/3b2/AR##/Vol00000/110234/APPFile/JW-AR##110234

J_ID: Z3X Customer A_ID: 11-0178.R1 Cadmus Art: AR21541 Date: 22-November-11 Stage: Page: 8

TABLE 1. Eye measurements for all specimens used in the regression analysis

ID	BL	Age	EL	EW	EH	CH	CW	LW	LH	LL	PND	CTC	CTP
102710-PV-Ea 33	11.9	A	46	72	70	17	30	–	–	–	–	–	–
080310-PV-Ea 05	14.9	A	59	74	77	24	35	–	–	–	–	–	–
070910-PV-Ea 01	12.7	A	50	69	73	24	35	–	–	–	–	–	–
091410-PV-Ea 19	12.5	A	46	73	71	21	32	–	–	–	24	1.4	1.8
092706-PV-Ea 11	7.7	C	46	66	64	27	38	–	–	–	–	–	–
081809-PV-Ea 21	5.8	C	44	57	53	21	32	–	–	–	–	–	–
092410-PV-Ea 24	7.4	C	31	59	57	23	33	–	–	–	–	–	–
072309-PV-Ea 07	5.9	C	41	66	64	21	35	–	–	–	–	–	–
082810-Pv-Ea 16	6.0	C	39	61	58	24	32	–	–	–	–	–	–
071610-Pv-Ea 03	6.5	C	38	61	59	22	35	–	–	–	–	–	–
081709-PV-Ea 19	6.7	C	44	60	58	22	29	–	–	–	–	–	–
090109-PV-Ea 40	6.2	C	35	61	56	20	33	–	–	–	–	–	–
081209-PV-Ea 18	8.0	C	41	68	67	22	32	–	–	–	–	–	–
092807-PV-Ea 19	6.9	C	33	59	56	22	30	–	–	–	–	–	–
101807-PV-Ea 41	7.8	C	41	64	65	24	32	–	–	–	–	–	–
080203-Pv-Ea 02	5.7	C	29	52	52	21	29	–	–	–	–	–	–
071210-PV-Ea 02	4.9	C	33	50	49	20	26	10	11	7	18	1.1	2.4
091309-Pv-Ea 48	5.2	C	28	56	55	20	28	–	–	–	–	–	–
101207-PV-Ea 37	7.2	C	37	61	60	20	26	–	–	–	–	–	–
170809-PV-Ea 20	5.8	C	28	55	51	23	29	–	–	–	–	–	–
082110-PV-Ea 10	5.2	C	34	55	50	21	30	–	–	–	–	1.4	2.0
081910-PV-Ea 09	6.3	C	38	59	56	22	28	–	–	–	–	–	–
090210-PV-Ea 17	7.3	C	46	63	60	22	33	–	–	–	–	–	–
092510-PV-Ea 24	6.1	C	34	56	53	18	24	–	–	–	–	–	–
081707-PV-Ea 09	5.3	C	31	55	50	20	30	–	–	–	–	–	–
082210-PV-Ea 11	4.9	C	34	55	54	22	28	–	–	–	–	–	–
101407-Pv-Ea 39	7.7	C	38	64	60	20	27	–	–	–	–	–	–
062909-Pv-Ea 01	5.5	C	31	60	54	21	30	–	–	–	–	–	–
082410-Pv-Ea 12	4.1	C	25	48	44	17	25	–	–	–	–	–	–

Body length in meters, all other measurements are in millimeters.
ID: identification number of the specimens; BL: body length; EL: eyeball length; EW: eyeball width; EH: eyeball height; CH: corneal height; CW: corneal width; LW: lens width; LH: lens height; LL: lens length; PND: posterior nodal distance; CTC: corneal thickness at the center; CTP: corneal thickness at the periphery. See Figure 1 for explanation of the measurements taken.

(*Dermochelys coriacea*), is also plausible for whales (Brudenall et al., 2008).

As in other cetaceans, in *Eubalaena australis* the blood irrigation in the eye is well-developed, particularly the ophthalmic rete. The presence of this rete has been extensive cited in published reports although its role remains unclear. Based on prominent vasculature and position of the ophthalmic rete, it has been suggested that it play a role in supplying the pressure needed in moving the eyeball outward (Bjerager et al., 2003). However, as the rete is not large enough to push the eyeball, and the vascular complex has neither the anatomic structure nor the pump mechanism required to retracting it, this idea has recently been questioned (Ninomiya and Yoshida, 2007). Other functions that have been linked to the ophthalmic rete include oxygen stores, temperature regulation, and improvement of visual performance. In a comprehensive analysis on the functional anatomy of the ocular circulatory system of the cetacean eye, Ninomiya and Yoshida (2007) concluded that the ophthalmic rete, as well as the vascular eye pattern as a whole, might function as a thermoregulatory system maintaining an appropriate operating temperature for the photoreceptors even in deep and cold aquatic environment. The ophthalmic rete might has the same general function as the other anastomotic networks of small arteries forming the rete mirabilis in the basicranial region of the skull, along the vertebral column and in the thoracic region. That is, to modulate and dampen fluctuations in the flow of blood to the central nervous system and also as oxygen storage (Nagel et al., 1968; Geisler and Luo, 1998). The peculiar ocular vascular pattern of cetaceans might also be for pooling blood in the eye to conserve oxygen during dives, and that the ophthalmic rete might play a role in a pressure-

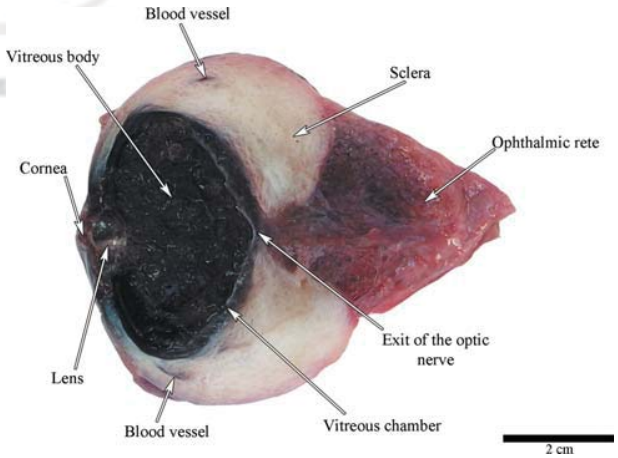

Fig. 7. Transverse section of the left eyeball (082110-PV-Ea10) showing the vitreous chamber with the vitreous body, lens, and the vascularization of the sclera.

COLOR

ID: selvarajn | Black Lining: [ON] | Time: 14:05 | Path: N:/3b2/AR##/Vol00000/110234/APPFile/JW-AR##110234

J_ID: Z3X Customer A_ID: 11-0178.R1 Cadmus Art: AR21541 Date: 22-November-11 Stage: Page: 9

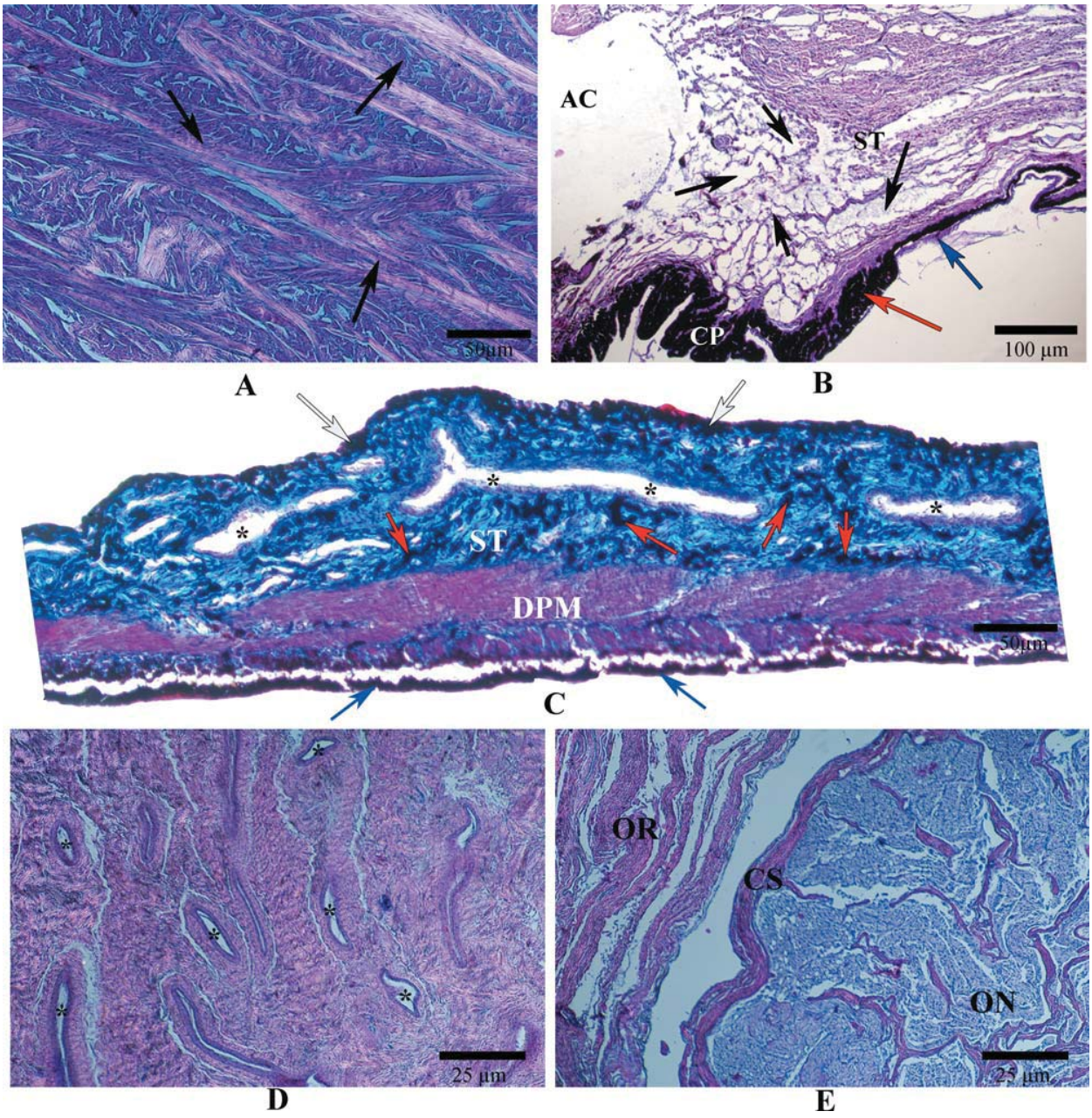

Fig. 8. **A:** Longitudinal section of the sclera composed of a large amount of collagen fibers (arrows) tightly packed and arranged in different directions to each other. H&E stain. **B:** Cross-section of the ICA illustrating the anterior chamber (AC), the sclerocorneal stroma (ST) with the large spaces of Fontana and trabecular meshworks (black arrows), and the ciliary processes (CP) composed of a thin inner epithelium layer of nonpigmented cell (blue arrow) and a thick outer layer with abundant melanocytes (red arrow). H&E stain. **C:** Cross-section of the iris. Note the outer limiting layer (white arrows), the thick stroma (ST) with abundant blood vessels (*) and melanocytes (red arrows) and the well-developed dilator papillae muscle (DPM) placed between the stroma and the inner iris epithelium (blue arrows). Masson's trichrome stain. **D:** median section through the ophthalmic rete showing the well-developed network of blood vessel (*) dispersed in abundant connective tissue. H&E stain. **E:** Median section of the optic nerve (ON) surrounded by a connective sheath (CS) and the ophthalmic rete (OR). H&E stain. Specimen number 080910-PV-Ea 06 (right eye).

damping effect on cetacean ocular circulation as well (Ninomiya and Yoshida, 2007). In addition, the warm eyeball may prevent the fat around the orbit from setting and therefore, fat fluidity could help in smooth eyeball movements (Ninomiya and Yoshida, 2007). In this context, in *E. australis*, the ophthalmic rete as well as the presence of periorbital fat surrounding the eyeball may act as a thermoregulatory system of a high and appropriate operating temperature, and thus increasing visual performance.

COLOR

J_ID: Z3X Customer A_ID: 11-0178.R1 Cadmus Art: AR21541 Date: 22-November-11 Stage: Page: 10

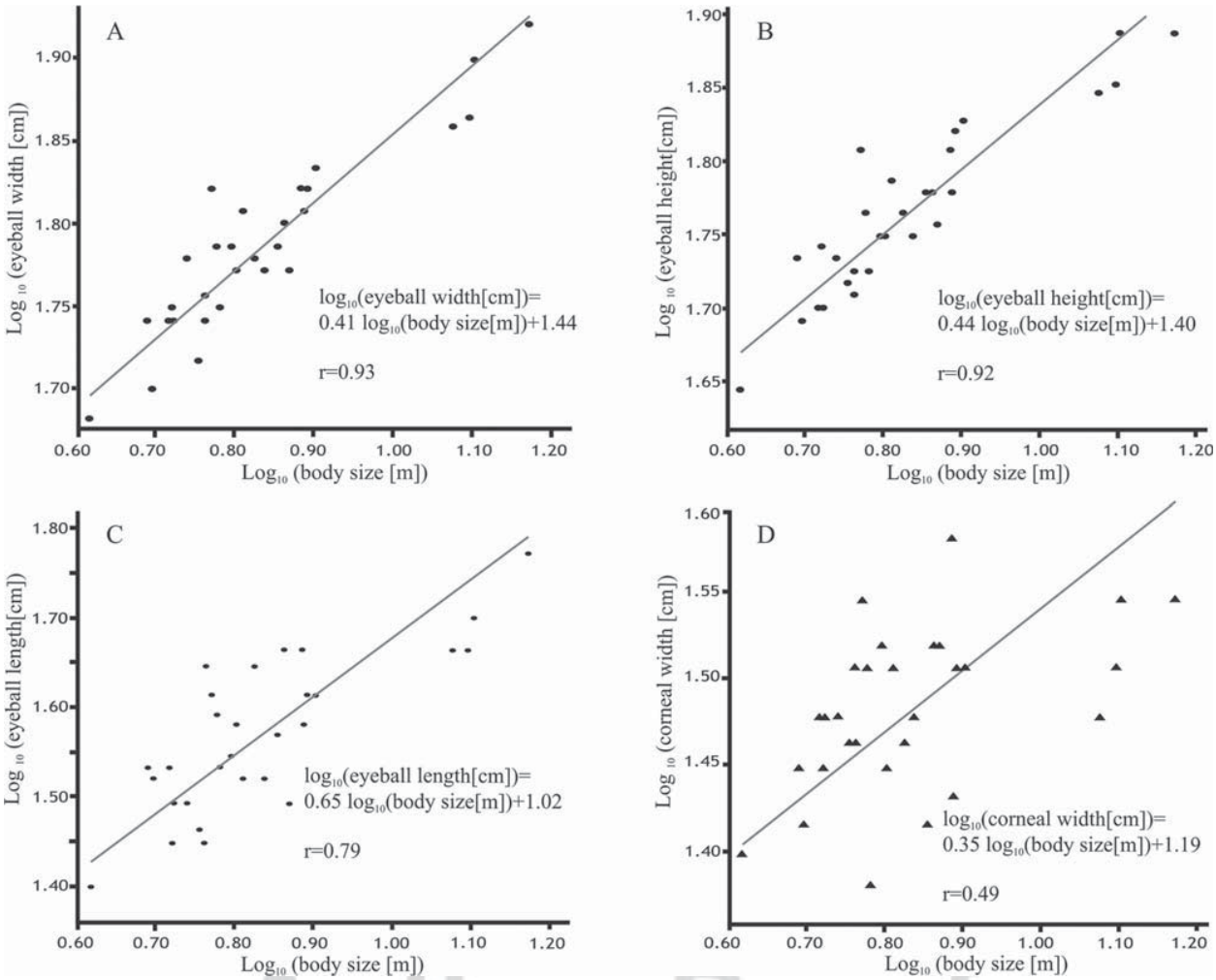

Fig. 9. Relationship between eye and cornea size and body length. **(A–D)** Scatter plots of 4 log-transformed linear measurements versus log-transformed body length.

TABLE 2. Results for SMA regression analysis for *Eubalaena australis* of eye variables (Y-variable) versus body length (X-variable; all variables are log_{10})

		Regression analysis				Correlation
Y-variable	*n*	*a* (slope)	*P*-value (*a*=1)	*b* (intercept)	*P*-value (uncorre)[a]	*r*[b]
Eyeball width	29	0.41	<0.001	1.44	<0.001	0.93
Eyeball height	29	0.44	<0.001	1.40	<0.001	0.92
Eyeball length	29	0.65	<0.001	1.02	<0.001	0.79
Corneal width	29	0.35	<0.001	1.19	0.006	0.49
Corneal height	29	0.33	<0.001	1.05	0.14 (NS)[c]	0.29

n: number of specimens.
[a]Value probability of no correlation.
[b]Pearson correlation coefficient.
[c]Statistically nonsignificant difference.

Histological analysis of the cetacean eyes as well as other marine mammals is scarce in the published reports. Hatfield et al. (2003) explored the structural pattern and function of the ICA in aquatic and terrestrial mammals, including the West Indian manatee (*Trichechus manatus*), short-finned pilot whale (*Globicephala macrorhynchus*), hippopotamus (*Hippopotamus amphibius*), and African elephant (*Loxodonta africana*). In the West Indian manatee, pilot whale, and hippopotamus the ICA is characterized by large space of Fontana unlike that of the African elephant. Another striking feature is the increased vascular supply within the ICA

ID: selvarajn | Black Lining: [ON] | Time: 14:06 | Path: N:/3b2/AR##/Vol00000/110234/APPFile/JW-AR##110234

in the manatee and the pilot whale dolphin contrasting with the small to moderate average of vessels within the ICA in the hippopotamus and the African elephant. The ICA pattern in *E. australis* is consistent with those of fully aquatic mammals in possessing a large space of Fontana as well as an increased vascular supply.

It has been suggested that a large space of Fontana indicates an increased importance of aqueous outflow by the uveoscleral route (Hatfield et al., 2003). This pattern in hippopotamus, manatees, dolphins, and whales indicates that it characterized fully aquatic as well as semiaquatic mammals (i.e., species with aquatic and aerial vision). Southern right whale, pilot dolphin, and the manatees also share the lack of ciliary body musculature and increased vasculature in the ciliary processes. The increase in vascular supply has been linked with the development of an alternative mechanism of lens accommodation to compensate the absence of ciliary musculature (Hatfield et al., 2003; Natiello and Samuelson, 2005).

The most striking difference between *E. australis* and *Balaena mysticetus* eye is related to the amount and distribution of periorbital fat. In *B. mysticetus*, the periorbital fat is distributed in three well-developed layers (external, middle, and inner layers), which can be identified both in calves and adults (Zhu et al., 2001), whereas in *E. australis*, the middle and deeper layers are poorly developed.

Lipids have multiple functions in cetaceans, such as thermoregulation, buoyancy control, streamlining, metabolic energy storage, locomotion (Struntz et al., 2004). In addition, highly specialized fat bodies in the dolphin heads serve to transmit and receive sound (Koopman and Zahorodny, 2008). In the particular case of periorbital fat, it has been proposed that the large amount of fat within the orbit is related to the protection of the eye from mechanical shock during retraction into the orbit, and/or to thermal insulation from low temperatures (Zhu et al., 2001). Bowhead whales inhabit polar waters in northern latitudes (between 80 and 60-degree angle N) and have the thickest bubbler layer of any baleen whale, which has been interpreted as an adaptation to the icy waters (Rugh and Shelden, 2009). Southern right whales occur in middle latitudes, between 20 and 60-degree angle S latitudes (Kenney, 2009). Besides, if the authors compare calf specimens of both southern right and bowhead whales with similar body sizes, the periorbital fat is significantly more abundant in bowhead whale calves (Zhu et al., 2001, Figure 5:735) than in the southern right whale. In *E. australis* calves, birth takes place in temperate waters (between 13 and −16°C; Kenney, 2009), whereas in *B. mysticetus*, it occurs in polar waters (Rugh and Shelden, 2009). Unlike bowhead whale calves, the southern right whale calves spend the early months in temperate waters growing and storing energy before their migration to the feeding grounds in higher latitudes (Best et al., 1993; Best, 1994). The variation in the abundance of the periorbital fat between these two species could be attributed to the different latitudinal ranges where they live; thus, physical constraints such as water temperature imposed by the environment could be determinants in the development of this dynamic tissue.

The bubbler layer that covers the external surface of the body in baleen whales does not present a homogeneous histological structure and composition between the innermost and the outermost layers (Ackman et al., 1975; Lockyer et al., 1984; Aguilar and Borrell, 1990). However, data on cetacean periorbital fat structure and distribution are extremely scarce in the published reports. Although Zhu et al. (2001) described the distribution of the fatty layers that surrounding the eyeball in *B. mysticetus*, they do not refer to the structure of these layers. As described in *E. australis*, field examination of a juvenile specimen of *Caperea marginata* (NMNZ 011345) stranded on New Zealand coast reveals a similar pattern of periorbital fat. In this specimen, the outermost layer is more tight and firm than the innermost. Also, the two inmermost layers were also identified in the eye of a fin whale *Balenoptera physalus* (Mónica R. Buono, pers. obs.).

From the two main functions have been proposed to the periorbital fat, that is, mechanical protection (during eye retraction or compression/expansion during diving) and/or thermal insulation, the more superficial layer has likely a structural role while the deeper fatty layers could be metabolically active and also related to thermoregulation, and their development may depend on lipid dynamics. The role in thermal insulation permit to explain the large difference in the amount of periorbital fat between *B. mysticetus*, inhabitant of polar waters, and its closely related *E. australis* inhabitant of more warm waters in the Southern Hemisphere. The uneven distribution of the periorbital fat around the eye observed in the adults could be related to differences in the metabolic activity of these layers as a consequence of different age, nutritional, or reproductive status of the individual. The reproductive cycle of southern right whales implies high energetic demands for the females, which depend on the energy stores, such as body fat and protein stores in muscle tissue (Oftedal, 1993, 2000). In *Balaenoptera physalus*, females the most dramatic changes in deposition or mobilization of lipids occur during the fasting and fattening cycles. These variances in lipid content are more active in the internal fatty layer and this variation depends on the reproductive status of the females (Aguilar and Borrell, 1990). In addition, Valenzuela et al. (2010) have demonstrated that interannual variations in the stable isotope concentrations between mothers and their calves could be associated with different levels of nutritional stress. This stress could be related to changes in the food abundance. Therefore, the females are not physically prepared to meet the energetic demands of reproduction and lactation and have to mobilize their own body reserves. Measurements of the blubber thickness in the body of these specimens provide for the Stranding Network at Península Valdés, reveal that those females with less amount of periorbital fat (070910-PV-Ea 01 and 091410-PV-Ea 19) also posses thinner body blubber layer. Although the authors do not know the reproductive status of these females in our sample when they died, the differences in the abundance of the periorbital and body fat suggest that the females were in different times of the reproductive cycle. Some of these females could have metabolized their lipid storage in response to different energetic demands. This hypothesis needs to be tested in the future; however, it is consistent with the reported distribution of structural and nonstructural fat within the cetacean blubber, that is, lipids in the superficial

J_ID: Z3X Customer A_ID: 11-0178.R1 Cadmus Art: AR21541 Date: 22-November-11 Stage: Page: 12

blubber are metabolically inert ("structural lipids") and the deepest layers are more metabolically active (Aguilar and Borrell, 1990; Struntz et al., 2004; Klanjscek et al., 2007). Another striking aspect related with the periorbital fat in *E. australis* is the pattern of fat deposition. Only in the largest calves were the deeper (inner) and medium fatty layers developed, with the inner layer being thicker than the medium layer. This pattern suggests that the inner layer was the first to be deposited. The decrease of periorbital fat observed in *E. australis* could imply a risk for thermal insulation, inhibiting retina and optic nerve warming, which in fact may affect vision. However, in the case of this species, the loss of a significant amount of periorbital fat does not necessarily introduce a trade-off with respect to visual performance as this decrease is documented when these whales inhabit in temperate waters of Península Valdés during their breeding season. The development of periorbital fat may be also beneficial in dealing with the generation of a flexible space to accommodate expansion or compression of neighboring structures during the accommodation of the eyeball in diving/ascent sequence.

The main differences in anatomy of the orbital region between mysticetes and odontocetes occur in the neighboring structures surrounding the eyeball, but not in the eyeball itself. Thus, in odontocetes, periorbital fat has not been reported. In addition, there are conspicuous differences in the development of the pterygoid sinus. In odontocetes, the pterygoid sinus are extensively developed, extending dorsally onto the frontal and sphenoid forming preorbital and postorbital lobes, while in mysticetes this sinus is less developed and restricted to the middle ear cavity (Fraser and Purves, 1960; Mead and Fordyce, 2009). The pterygoid sinus is associated with a network of blood vessels which fill it with blood during diving to the same degree the increasing hydrostatic pressure diminishes the air volume in the middle ear (Cranford et al., 2008). The presence of large pterygoid sinuses of odontocetes has been interpreted as an essential adaptation for maintaining acoustic isolation and auditory acuity of the ears at depth and protection of the middle ear structures during diving (Fraser and Purves, 1960; Cranford et al., 2008). However, functionality of these air sinuses within the orbit has not been explored. A putative function of the air sac in the orbit of odontocetes is, as the periorbital fat of mysticetes, the protection of the eyeball during diving and allows the accommodation of surrounding structures. However, to test this hypothesis is beyond the scope of the present contribution.

Linear measurements of the eye showed that in *E. australis*, there is a correlation of the eye size with the body length. The body length correlates best with eye width and height, and least with the length (i.e., axial length). The axial length could be interpreted as a proxy of the posterior nodal region, and it is this length that relates to visual capabilities as retinal magnification factor, focal length, and acuity (Hughes, 1977; Howland et al., 2004). However, the axial length, as well as the eye width and eye height, is overestimated due to the thick sclera. In the sample analyzed, the cornea size measured as the corneal width and height, has a low correlation or no correlation with the body length, respectively.

The size of the eye and lens and the estimated *f*-number suggest that the optical sensitivity of the *E. australis* eye is relatively low. The estimated *f*-number is 2 and 1.81 when the diameter of the lens is measured rostro-caudally and dorso-ventrally, respectively. These values are similar to those of marine turtles *Chelonia mydas* ($f = 2.4$, Mäthger et al., 2007) and *Dermochelys coriacea* ($f = 2.3$, Brudenall et al., 2008), but higher than those of diving fishes such as blue marlins *Makaira nigricans* ($f = 1.6$, Fritsches et al., 2005). Among marine mammals, the only published data correspond to elephant seal *Mirounga* spp., in which the estimated *f*-number was 1.18–1.48 (Humphries and Ruxton, 2002). Mass and Supin (1997, 2002) measured optical parameters of gray whales *Eschrichtius robustus* and belugas *Delphinapterus leucas* including the PND and the antero-posterior and dorso-ventral diameters lens. These data result in an estimated *f*-number of 2.56 and 1.97 (for antero-posterior and dorso-ventral lens diameters, respectively) for the *E. robustus* eye, and of 1.90 and 1.67 for the *D. leucas* eye (for antero-posterior and dorso-ventral diameters, respectively). However, caution had to be taken in interpreting *f*-number as a proxy of eye sensitivity. Available data of optical parameters of aquatic animals such as the *f*-number are, up to date, scarce. The estimated *f*-number values change depending upon assumptions about pupil diameter, which in turn is estimated on the lens size. Proper lens measurements are very difficult to obtain and, in most of the cases, the lack of access to fresh tissue means that measurements of the lens are undertaken on frozen material and shrinkage affects results. As a consequence, in most of the contributions, the *f*-number could be estimated for few (or even a single) specimens.

As has been discussed, the study of the eye anatomy provides useful information not only about the visual capabilities of the mysticete but also their ecological aspects. It has been established that, especially in the published reports from the last century, baleen whales have poor vision; this assumption was based upon wrong observations/interpretations of the baleen whale eye anatomy (Weber, 1886; Pütter, 1903, Walls, 1942). However, new anatomical findings are not consistent with this assumption (Murayama et al., 1992; Mass and Supin, 1997; Zhu et al., 2000, 2001) and they have demonstrated important adaptations in the visual system of baleen whales both to the aquatic and aerial environment (Mass and Supin, 2007). More studies that explore the anatomy and optical capabilities of other mysticetes are needed to reject or accept this statement.

ACKNOWLEDGEMENTS

We are extremely grateful for the personal and volunteers of the Stranding Network at Península Valdés (V. Rowntree, M. Sironi, M. Uhart, A. Chirife, L. Bandieri, M. Di Martino, and Lucas Beltramino) who collected and donated samples for this study. The authors also express our sincere thanks to A. Chirife, M. Di Martino, J. Briguglio, J. Rua, L. F. Britos, N. V. Barloa, M. Reparaz, L. Hardtke, V. H. Ruiz, J. Orgeira, and E. Gonzalez for their valuable help, support, and encouragement during dissections in the field and in the lab. M. Sironi (Instituto de Conservación de Ballenas) and L. Valenzuela (University of Utah) are thanked for the published report assistance. Thanks to personal of Stranding Network at Península Valdés to provide the

ID: selvarajn | Black Lining: [ON] | Time: 14:06 | Path: N:/3b2/AR##/Vol00000/110234/APPFile/JW-AR##110234

photograph in Fig. 2A and the information of blubber thickness of adult specimens. The authors are particularly grateful to N. Luján from the histological service of Centro Nacional Patagónico for the excellent job in the preparation of the sample tissue for the histological studies and C. Pastor (Centro Nacional Patagónico) for the histological photographs. The authors would like to thank R. E. Fordyce (Department of Geology, University of Otago) and A. van Helden (Museum of New Zealand Te Papa Tongarewa) for allowing Mónica R. Buono to participate in the dissection of a *Caperea* specimen in New Zealand. The authors gave thanks to J. S. Reidenberg (Mount Sinai School of Medicine) to provide access to Mónica R. Buono to examinate eyes samples of rorqual's whales in her care in the Mount Sinai School of Medicine, New York. The authors wish to thank N. D. Pyenson (National Museum of Natural History, Smithsonian Institution), R.N. P. Goodall (Museo Acatushún de Aves y Mamíferos Marinos Australes, AMMA), and A. Formoso (CENPAT-CONICET) for their helpful comments and for help with English version of the manuscript. M. T. Dozo (CENPAT-CONICET) is thanked for her assistance during this study. The authors are grateful to the anonymous reviewers and editor (Prof. Jeffrey Laitman), their suggestions greatly improved the quality of this article. Field work was conducted under permits from Dirección de Fauna y Flora Silvestre and Secretaria de Turismo y Areas Protegidas del Organismo Provincial de Turismo, Chubut Province. This article is part of a doctoral research of Mónica R. Buono at Universidad de La Plata and Centro Nacional Patagónico (CENPAT-CONICET).

LITERATURE CITED

Ackman RG, Hingley JH, Eaton CA, Sipos JC, Mitchell ED. 1975. Blubber fat deposition in Mysticeti whales. Can J Zool 53: 1332–1339.

Aguilar A, Borrell A. 1990. Patterns of lipid content and stratification in the blubber of fin whales (*Balaenoptera physalus*). J Mammal 71:544–554.

Alexander RM. 1985. Body support, scaling and allometry. In: Hildebrand M, Bramble DM, Liem KF, Wake DB, editors. Functional vertebrate morphology. Cambridge Harvard University Press. p 27–37.

Baker CS, Patenaude NJ, Bannister JL, Robins J, Kato H. 1999. Distribution and diversity of mtDNA lineages among southern right whales (*Eubalaena australis*) from Australia and New Zealand. Mar Biol 134:1–8.

Best PB. 1990. Trends in the inshore right whale population off South Africa, 1969–1987. Mar Mammal Sci 6:93–108.

Best PB, Payne R, Rowntree V, Palazzo JT, Both MD. 1993. Long-range movements of South Atlantic right whales *Eubalaena australis*. Mar Mammal Sci 9:227–234.

Best PB. 1994. Seasonality of reproduction and the length of gestation in southern right whales, *Eubalaena australis*. J Zool 232: 175–189.

Best PB, Schell DM. 1996. Stable isotopes in southern right whale (*Eubalaena australis*) baleen as indicators of seasonal movements, feeding and growth. Mar Biol 124:483–494.

Best PB. 1997. Whale Watching in South Africa. The Southern Right Whale. 2nd ed. Pretoria: Mammal Research Institute, University of Pretoria.

Bjerager P, Heegaard S, Tougaard J. 2003. Anatomy of the eye of the Sperm whale (*Physeter macrocephalus L.*). Aquat Mammal 29:31–36.

Brudenall DK, Schwab IR, Fritsches KA. 2008. Ocular morphology of the Leatherback sea turtle (*Dermochelys coriacea*). Vet Ophthalmol 11:99–110.

Cranford T, McKenna M, Soldeville M, Wiggins S, Goldbogen J, Shadwick R, Krysl P, St. Leger J, Hildebrand J. 2008. Anatomic geometry of sound transmission and reception in Cuvier's beaked whale (*Ziphius cavirostris*). Anat Rec 291:353–378.

Dawson WW, Brindford LA, Perez JM. 1972. Gross anatomy and optics of the dolphin eye (*Tursiops truncatus*). Cetology 10:1–12.

Dawson WW. 1980. The cetacean eye. In: Herman LM, editor. Cetacean behavior. New York: John Wiley and Sons. p 53–100.

Dral ADG. 1983. The retinal ganglion cells of *Delphinus delphis* and their distribution. Aquat Mammals 10:57–68.

Emerson SB, Bramble DM. 1993. Scaling, allometry and skull design. In: Hanken J, Hall BK, editors. The skull. Chicago: University of Chicago Press. p 384–416.

Fraser FC, Purves PE. 1960. Hearing in cetaceans: evolution of the accessory air sacs and the structure and function of the outer and middle ear in recent cetaceans. Br Mus (Nat Hist) Bull Zool 7:1–140.

Fritsches KA, Brill RW, Warrant EJ. 2005. Warm eyes provide superior vision in swordfishes. Curr Biol 15:55–58.

Geisler JH, Luo Z. 1998. Relationships of Cetacea to terrestrial Ungulates and the evolution of cranial vasculature in Cete. In: Thewissen JGM, editor. The emergence of the whales. Evolutionary patterns in the origin of Cetacea. New York: Plenum Press. p 163–212.

Goodall RNP, Galeazzi AR. 1986. Recent sightings and strandings of southern right whales off subantarctic South America and the Antarctic Peninsula. Report to the International Whaling Commission (special issue) 10:173–176.

Hatfield JR, Samuelson DA, Lewis PA, Chisholm M. 2003. Structure and presumptive function of the iridocorneal angle of the West Indian manatee (*Trichechus manatus*), short-finned pilot whale (*Globicephala macrorhynchus*), hippopotamus (*Hippopotamus amphibius*), and the African elephant (*Loxodonta africana*). Vet Ophthalmol 6:35–43.

Herman LM, Peacock MF, Yunker MP, Madsen CJ. 1975. Bottlenosed dolphin: double-split pupil yields equivalent aerial and underwater diurnal acuity. Science 189:650–652.

Howland HC, Merola S, Basarab JR. 2004. The allometry and scaling of the size of vertebrate eyes. Vis Res 44:2043–2065.

Hughes A. 1977. The topography of vision in mammals of contrasting life style: comparative optics and retinal organization. In: Crescitelli F, editor. The visual system in vertebrates, Vol. VII/5. Berlin: Springer Verlag. p 613–756.

Humphries S, Ruxton GD. 2002. Why did some ichthyosaurs have such large eyes? J Exp Biol 205:439–441.

International Whaling Commission. 2001. Report of the workshop on the comprehensive assessment of right whales: a worldwide comparison. J Cetacean Res Manage Special Issue 2:1–60.

Kastelein RA, Zweypfennig RCVJ, Spekreijse H. 1990. Anatomical and histological characteristics of the eyes of a month-old and an adult harbor porpoise (*Phocoena phocoena*). In: Thomas JA and Kastelein RA editors. Sensory abilities of Cetaceans. New York: Plenum. p 463–480.

Klanjscek T, Nisbet RM, Caswell H, Neubert MG. 2007. A model for energetic and bioaccumulation in marine mammals with applications to the right whale. Ecol Appl 17:2233–2250.

Kenney RB. 2009. Right whales. In: Perrin WF, Würsing B, Thewissen JGM, editors. Encyclopedia of marine mammals. San Diego, CA: Academic Press. p 962–969.

Koopman HN, Zahorodny ZP. 2008. Life history constrains biochemical development in the highly specialized odontocete echolocation system. Proc R Soc B 275:2327–2334.

Lockyer CH, McConnell LC, Waters TD. 1984. The biochemical composition of fin whale blubber. Can J Zool 62:2553–2562.

Mass AM, Supin AYa. 1989. Distribution of ganglion cells in the retina of an Amazon river dolphin *Inia geoffrensis*. Aquat Mammal 15:49–56.

Mass AM, Supin AYa. 1995. Ganglion cells topography of the retina in the bottlenosed dolphin, *Tursiops truncatus*. Brain Behav Evol 45:257–265.

Mass AM, Supin AYa. 1997. Ocular anatomy, retinal ganglion cell distribution, and visual resolution in the gray whale, *Eschrichtius gibbosus*. Aquat Mammal 23:17–28.

Mass AM, Supin AYa. 2002. Visual field organization and retinal resolution of the beluga, *Delphinapterus leucas* (Pallas). Aquat Mammal 28:241–250.

Mass AM, Supin AYa. 2007. Adaptive features of aquatic mammals' eye. Anat Rec 290:701–715.

Mäther LM, Litherland L, Fritsches KA. 2007. An anatomical study of the visual capabilities of the green turtle, *Chelonia mydas*. Copeia 1:169–179.

Matthews LH. 1938. Notes on the southern right whale, *Eubalaena australis*. Discov Rep 17:169–182.

Mead J, Fordyce RE. 2009. The therian skull: a lexicon with emphasis on odontocetes. Smithson Contrib Zool 627:1–261.

Murayama T, Somiya H, Aoki I, Ishii T. 1992. The distribution of ganglion cells in the retina and visual acuity of minke whale. Nippon Suissan Gakkaishi 58:1057–1061.

Nagel EL, Morgane PJ, McFarland WL, Galliano RE. 1968. Rete mirabile of dolphin: its pressure-dampening effect on cerebral circulation. Science 161:898–900.

Natiello M, Samuelson D. 2005. Three-dimensional reconstruction of the angioarchitecture of the ciliary body of the West Indian manatee (*Trichechus manatus*). Vet Ophthalmol 8:367–373.

Ninomiya H, Yoshida E. 2007. Functional anatomy of the ocular circulatory system: vascular corrosion casts of the cetacean eye. Vet Ophthalmol 10:231–238.

Oftedal OT. 1993. The adaptation of milk secretion to the constraints of fasting in bears, seals, and baleen whales. J Dairy Sci 76:3234–3246.

Oftedal OT. 2000. Use of maternal reserves as a lactation strategy in large mammals. Proc Nutr Soc 59:99–106.

Ohsumi S, Kasamatsu F. 1986. Recent off-shore distribution of the southern right whale in summer, Appendix. Natural marking of right whales. Report to the International Whaling Commission (special issue) 10:185.

Patenaude NJ, Baker CS. 2001. Population status and habitat use of southern right whales in the sub-Antarctic Auckland Islands of New Zealand. J Cetacean Res Manage (special issue) 2:111–116.

Payne R, Brazier O, Dorsey EM, Perkins JS, Rowntree VJ, Titus A. 1983. External features in southern right whales (*Eubalaena australis*) and their use in identifying individuals. In: Payne R, editor. Communication and behavior of whales. Colorado: AAAS Selected Symposia Series 76, Westview Press. p 371–445.

Payne R. 1986. Long term behavioral studies of the southern right whale (*Eubalaena australis*). Report to the International Whaling Commission (special issue) 10:161–167.

Pilleri G, Wandeler A. 1964. Ontogenese und functionelle morphologie der auges des finnwals *Balaenoptera physalus L.* (Cetacea, Mysticeti, Balaenopteridae). Acta Anat 57 (Suppl 50):1–74.

Pütter A. 1903. Die Augen der Wassersaugetiere. Zool Jahrb Abth Anat Ontog Thiere 17:99–402.

Reeb D, Best PB, Kidson SH. 2007. Structure of the integument of southern right whales, *Eubalaena australis*. Anat Rec 290: 596–613.

Rowntree VJ, Valenzuela LO, Fraguas PF, Seger J. 2008.Foraging behaviour of southern right whales (*Eubalaena australis*) inferred from variation of carbon stable isotope ratios in their baleen. Report to the International Whaling Commission SC/60/ BRG23.

Rugh DJ, Shelden KEW. 2009. Bowhead whale. In: Perrin WF, Würsing B, Thewissen JGM, editors. Encyclopedia of marine mammals. San Diego, CA: Academic Press. p 131–132.

Struntz DJ, Mclellan WA, Dillaman RM, Blum JE, Kucklick JR, Pabst DA. 2004. Blubber development in bottlenose dolphins (*Tursiops truncates*). J Morphol 259:7–20.

Townsend CH. 1935. The distribution of certain whales as shown by logbook records of American whaleships. Zoologica 19: 1–50.

Valenzuela LO, Sironi M, Rowntree V, Seger J. 2009. Isotopic and genetic evidence for culturally inherited site fidelity to feeding grounds in southern right whales (*Eubalaena australis*). Mol Ecol 18:782–791.

Valenzuela LO, Sironi M, Rowntree V. 2010. Interannual variation in the stable isotope differences between mothers and their calves in southern right whales (*Eubalaena australis*). Aquat Mammal 36:138–147.

Vasilyevskaya, GI. 1988 The eye of the minke whale. I. General structure and the sclera. Vestnik Zool 5:67–72.

Waller G. 1982. Retinal ultrastructure of the Amazon river dolphin (*Inia geoffrensis*). Aquat Mammal 9:17–28.

Walls GL. 1942. The vertebrate eye and its adaptive radiation. New York: Hafner.

Warton DI, Wright IJ, Falster DS, Westoby M. 2006. Bivariate line-fitting methods for allometry. Biol Rev Camb Philos Soc 81: 259–291.

Weber M. 1886. Studien über Säugethiere. Ein Beitrag zur Frage nach den Ursprung der Cetaceen. Jena 132–142. AQ5

Zhu Q, Hillmann DJ, Henk WG. 2000. Observations on the muscles of the eye of the bowhead whale, *Balaena mysticetus*. Anat Rec 259:189–204.

Zhu Q, Hillmann DJ, Henk WG. 2001. Morphology of the eye and surrounding structures of the bowhead whale, *Balaena Mysticetus*. Mar Mammal Sci 17:729–750.

Zhu Q, Yamada TK, Xiang L. 2008. The structures of eye and surrounding tissues of Longman's beaked whale, *Indopacetus pacificus*. Chin J Ocean Limn 26:219–221.

AQ1: Please confirm that all author names are OK and are set with first name first, surname last.

AQ2: Please confirm that all affiliations are OK and are set with order.

AQ3: The institutional abbreviation "(NMNZ) Museum of New Zealand Te Papa Tongarewa, New Zealand" has been moved to the abbreviation list from the text. Please confirm if this is fine.

AQ4: Please cite Figure 6A inside the text.

AQ5: Please provide volume number for "Weber, 1886."